Sains Malaysiana 54(8)(2025): 1889-1900
http://doi.org/10.17576/jsm-2025-5408-02

Seismotectonic Characteristics of the Cugenang Fault, Cianjur, West Java, Based on *a*-Value, *b*-Value, Seismic Moment and Satellite Gravity (Earthquake Data of 2008 - 2023)

(Ciri Seismotektonik Sesar Cugenang, Cianjur, Jawa Barat, Berdasarkan Nilai *a*, Nilai *b*, Momen Seismik dan Graviti Satelit (Data Gempa Bumi 2008 - 2023))

ATIN PRIHATINI[1], RINA DWI INDRIANA[2,*], AGUS SETYAWAN[2] & MUHAMMAD FAHMI[2]

[1]*Physics Undergraduate, Department of Physics, Faculty of Science and Mathematics, Diponegoro University, Semarang, Indonesia*
[2]*Department of Physics, Faculty of Science and Mathematics, Diponegoro University, Semarang, Indonesia*

Received: 13 February 2025/Accepted: 26 May 2025

ABSTRACT

The formation of fault in Cugenang, Cianjur Regency, West Java, caused an earthquake on 21 November 2022, with a magnitude of 5.6 SR, resulting in significant losses and casualties. The orientation of the Cugenang fault is N 347° E, dip 82.8°, depth 10 - 11 km, and a dextral strike-slip mechanism. This research aims to analyze the seismotectonic activity in the Cianjur area using *a*-value, *b*-value, seismic moment, and gravity field anomaly data. The processing of the *b*-value, *a*-value, and seismic moment was conducted using earthquake data from the Indonesia Meteorology and Geophysics Agency's website, which includes longitude, latitude, magnitude, and earthquake depth (1 January 2008 - 28 February 2023). Gravity field anomalies were processed using GGMplus satellite data. The results indicate that residual gravity anomaly values and seismic moments are inversely proportional to the *a*-value and *b*-value. The seismic moment values range from 12.2 to 14.7, the b-value from 0.2 to 1, the *a*-value from 1.1 to 2.1, and the residual gravity anomaly is -16 mGal to 26 mGal. The earthquake's epicenters were distributed north of the Cimandiri fault in the Rajamandala segment, coinciding with the location of the Cugenang fault. The average earthquake depth ranged from 10 km to 20 km, suggesting that the earthquakes occurred in young volcanic rocks. The presence of active faults and brittle volcanic rocks makes the area around Cianjur prone to earthquakes and increases the potential for additional new faults.

Keywords: Characteristics; Cugenang; fault; new; seismotectonic

ABSTRAK

Pembentukan sesar di Cugenang, Kabupaten Cianjur, Jawa Barat, menyebabkan gempa bumi pada 21 November 2022 dengan kekuatan 5.6 SR yang mengakibatkan kerugian dan kehilangan jiwa yang besar. Orientasi sesar Cugenang ialah N 347° E, kemiringan 82.80°, kedalaman 10 - 11 km dan mekanisme gelinciran dekstral. Penyelidikan ini bertujuan untuk menganalisis aktiviti seismotektonik di kawasan Cianjur menggunakan data nilai *a*, nilai *b*, momen seismik dan anomali medan graviti. Pemprosesan nilai *b*, nilai *a* dan momen seismik dijalankan menggunakan data gempa bumi daripada laman web Agensi Meteorologi dan Geofizik yang merangkumi longitud, latitud, magnitud dan kedalaman gempa bumi (1 Januari 2008 - 28 Februari 2023). Anomali medan graviti diproses menggunakan data satelit GGMplus. Keputusan penyelidikan menunjukkan bahawa anomali graviti sisa dan nilai momen seismik adalah berkadar songsang dengan nilai *a* dan *b*. Nilai momen seismik berkisar antara 12.2 hingga 14.7, nilai *b* dari 0.2 hingga 1, nilai *a* dari 1.1 hingga 2.1 dan anomali graviti sisa -16 mGal hingga 26 mGal. Pusat gempa bumi tersebar di utara bahagian Rajamandala Sesar Cimandiri, bertepatan dengan lokasi Sesar Cugenang. Purata kedalaman gempa bumi berkisar antara 10 km hingga 20 km, ini menunjukkan bahawa gempa bumi berlaku di batuan gunung berapi muda. Kehadiran sesar aktif dan batuan gunung berapi yang rapuh menjadikan kawasan sekitar Cianjur terdedah kepada gempa bumi dan meningkatkan potensi penambahan sesar baharu.

Kata kunci: Baharu; ciri; Cugenang; seismotektonik; sesar

INTRODUCTION

The subduction of the Indo-Australian plate ranges from 100-200 km below the surface and 600 km north of Java (Shohaya et al. 2013). In the southern part of Java Island, the movement of the Indo-Australian plate towards the north collides with the relatively stationary Eurasian plate, while in the Sumatra region, the movement of the plate is relatively oblique towards the northeast. This makes the

regional tectonic situation in the southern region of western Java become a plate subduction area deflected around the southwest of the Sunda Strait. As a result, the regional tectonic situation in the south of west Java is more complex than in other parts of Java (Murjaya 2021). The subduction bending zone is a trigger zone for shallow earthquakes with large magnitudes that can trigger tsunamis. The subduction zone also causes the West Java region to have many volcanoes and pass by local faults.

Seismic activity in West Java often occurs because West Java is located in an active volcanic region, plate subduction zone, and Sunda Strait oblique zone (Murjaya 2021). The oblique zone is a zone that can trigger high-scale shallow earthquakes, which can trigger tsunamis on the coast of the Sunda Strait. The moving plate will press in all directions and layers. Large and continuous pressure will accumulate energy in all intersecting planes. Each plane has a different level of pressure/stress resistance. If the accumulated energy is in a stress-prone plane/layer, it will trigger an earthquake. In addition to earthquakes, energy release can trigger the movement of other geological structures, one of which is a fault. Faults can be categorized into major and minor faults. Major faults are the first to occur and stretch long across an area. The movement of the major fault causes the formation of minor faults along the major fault line. Brittle rock layers around major faults can contribute to the formation of minor faults. Brittle rocks generally cannot withstand pressure (Holtkamp & Brudzinski 2014).

In West Java, several major faults, including the Cimandiri fault. The Cimandiri fault is a fault that runs west-east in the southern region of West Java. One of the regencies traversed by the Cimandiri fault is the Cianjur Regency. History records earthquake activity in Cianjur occurred in 1844, 1912, 1968, 1982, and 2000, with an average magnitude of 5 SR (Viesser 1922). Seismic activity can also be generated by volcanic activity. Seismic records indicate that volcanic earthquakes magnitude 1 - 2 have occurred in the Cianjur and Sukabumi regencies. Mt. Pangrango and Mt. Gede in the Cianjur and Sukabumi regencies are the closest recorded sources of volcanic earthquakes. Mt. Pangrango and Mt. Gede are active volcanoes, therefore volcanic activity still occurs (Indriana et al. 2024).

On 21st November 2022, there was a 5.6 SR earthquake in Cianjur, West Java. The Ciamjur earthquake killed 162 people, 326 people were injured, and 13,784 people were displaced. Analysis of the focal mechanism, the distribution of aftershocks, satellite images, and aerial photographs, and detailed field surveys conducted by the Indonesian Agency for Meteorological, Climatological and Geophysics (BMKG) indicate that the Cianjur earthquake was caused by tectonic activity. The Cianjur earthquake was caused by a new fault that passed through Cugenang. The distribution pattern and characteristics of surface rupture, the distribution of landslide points, morphological alignment, and the distribution pattern of building damage indicate that the new Cugenang fault caused it. According to the Indonesian Agency for Meteorological, Climatological and Geophysics (BMKG) survey, the Cugenang Fault is a new fault with an orientation N 347° E, dip 82.8°, depth 10 - 11 km, length 19 km, and a dextral strike-slip mechanism (Daryono 2022). After an earthquake, energy is distributed radially, changing rock stress levels and seismic activity around the epicenter. The earthquake activity that occurs can trigger the emergence of new faults due to rock fragility. Therefore, it is necessary to study seismicity in the Cianjur area as part of disaster mitigation activities.

Seismicity identification can be done by calculating the *b*-value and *a*-value. *b*-value and *a*-value are calculated by applying the Gutenberg-Richter relationship (Wiemer, McNutt & Wyss 1998). The advantage of *b*-value is that it can quantitatively determine seismicity in a region based on statistics. The statistical calculation of seismicity uses earthquake occurrence data in an area (Mogi 1963). In addition to the *b*-value, subsurface analysis can use gravity and seismic moment data. The relationship between the three parameters (*b*-value, seismic moment, and gravity anomaly) is important for analyzing rock stress in areas of frequent earthquakes. If the relationship between the parameters is appropriate, it supports the accuracy and analysis of the *b*-value in the area (Bora et al. 2018).

Scholtz (1968) researched the relationship between the *b*-value and seismic moment, while Khan and Chakraborty (2007) researched the relationship between the *b*-value and Bouguer gravity anomaly. The results obtained show that seismic moment and Bouguer gravity anomaly have an inverse relationship with the *b*-value. The seismic moment can describe the variation of stress under the surface of an area (Aki 1966), while the Bouguer gravity anomaly can describe the heterogeneity of rocks that affect the stress under the Earth's surface, assuming that variations in lithospheric density can cause earthquakes (Sarkarinejad, Zadeh & Webster 2013). Seismicity research in the West Java region shows that the West Java region is classified as an area that has high seismicity (Hilmi 2019; Prananda, Zera & Sunarya 2022), this research only focuses on the *b*-value. The utilization of *a*-value, *b*-value, seismic moment, and Bouguer gravity anomaly can be considered in the study of earthquake activity and hazard estimation in tectonically active areas.

Based on this description, research with 4 parameters, spatial variation of *a*-value, *b*-value, seismic moment, and Bouguer gravity anomaly, has not been used to analyze seismicity in West Java, especially around the Cianjur area. The purpose of this study was to evaluate the relationship between heterogeneity and the stress level of rocks to earthquakes. This study focuses on the *b*-value, seismic moment, and residual gravity anomaly in the study area and ignores the volcanic contribution in the study area. The results of this study are expected to provide a discourse for future disaster mitigation activities related to the potential formation of faults in West Java.

MATERIALS AND METHODS

The research area is centered around the Cianjur region, located between 6.50°-7.10° N latitude and 106.60°-107.40° E longitude. The study area is approximately 88.17 km × 66.73 km, covering a total area of 5,884.33 km². It includes five administrative regions: Bogor Regency, Bogor City, Cianjur Regency, Sukabumi Regency, and Sukabumi City. The boundaries between these regencies and cities within the study area are illustrated in Figure 1.

GEOLOGY

The subduction bending zone acts as a trigger for shallow earthquakes with large magnitudes, which can lead to tsunamis. This subduction zone also contributes to the presence of numerous volcanoes in the West Java region and intersects with local faults. The geological setting of the West Java region is divided into four zones: the North Java Zone, the Central Volcano Zone, the Bogor Zone, and the Southern Mountain Zone (Figure 1).

The interaction between the Indo-Australian and Eurasian plates has resulted in a geological setting characterized by numerous volcanoes, including Mt. Pangrango. The rocks surrounding Mt. Pangrango are divided into Tertiary and Quaternary rocks. Mt. Pangrango is located within the Central Volcano Zone and is adjacent to the Bogor Zone. The rocks in the Bogor Zone are predominantly sedimentary and carbonate, with interspersed alluvium deposits. Sedimentary rocks include limestone, sandstone, tuffaceous clay, breccia, conglomerate, and marl. Carbonate rocks comprise reef limestone, passive limestone, clastic limestone, and marl. Intrusive rocks in this area consist of intermediate plagioclase and andesite. The ages of the rocks in the Bogor Zone vary significantly, with the youngest being Holocene volcanic rocks and alluvium, and the oldest being Oligo-Miocene sedimentary rocks (Ratman & Gafoer 1998). In the Central Volcano Zone, the rocks are primarily volcanic, interspersed with alluvium, lake deposits, reef limestone, intrusive rocks, and sedimentary rocks. The volcanic rocks include lava, breccia, tuff, and loose lava deposits, extending from west to east across Java Island. The lake deposits in this area are composed of tuffaceous clays and pebbles, while the intrusive rocks are basaltic. The youngest rocks in the Central Volcano Zone are Holocene volcanic rocks, reef limestone, alluvium, lake deposits, and Holocene intrusive rocks, while the oldest are Neogene volcanic rocks (Ratman & Gafoer 1998).

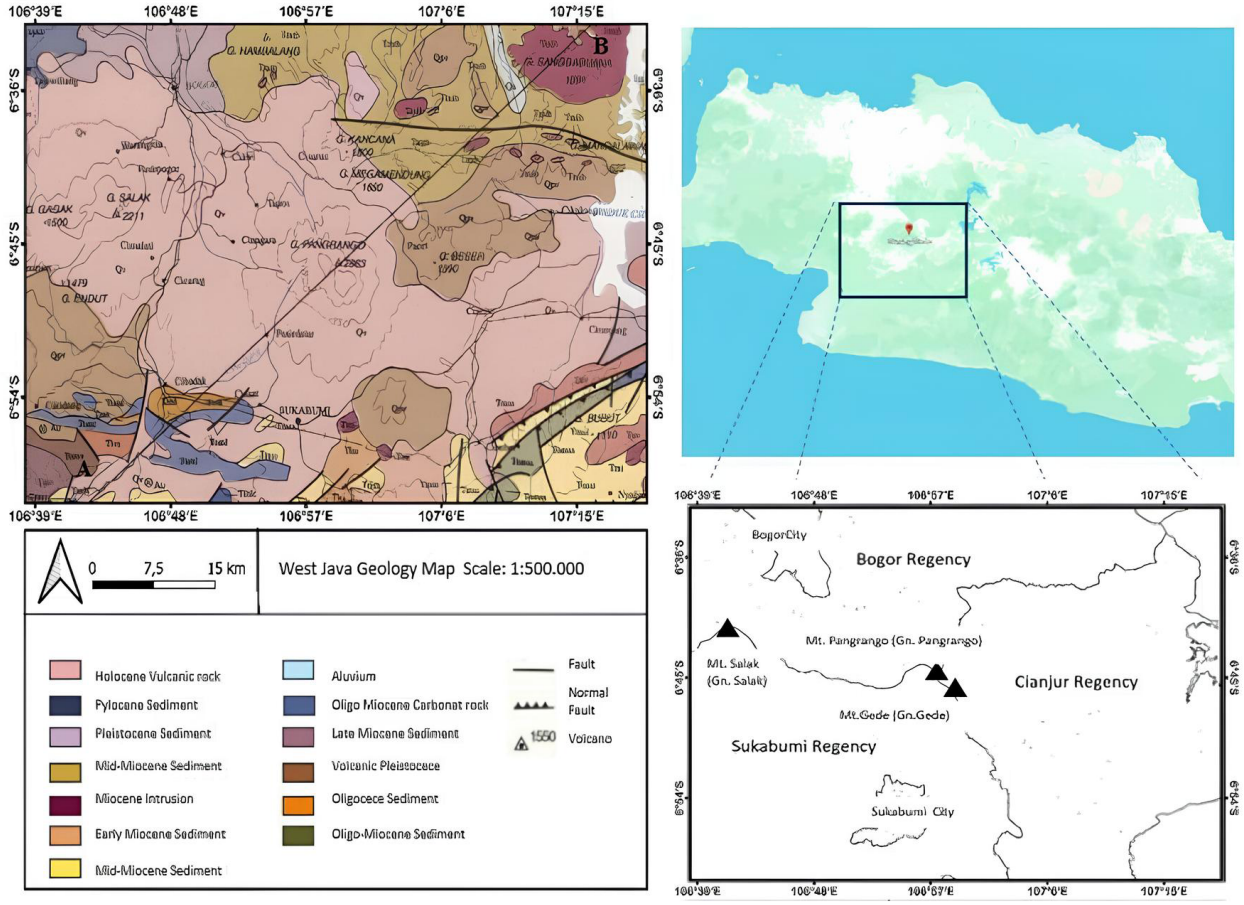

FIGURE 1. Research area

DATA

The data used in this study are secondary data, including earthquake data from the Indonesian Agency for Meteorological, Climatological and Geophysics website (https://www.bmkg.go.id/) and the free-air gravity anomaly satellite data from the GGMplus website (published by Curtin University) (Hirt et al. 2014). Using secondary data is an effective approach to developing analyses using available resources. The earthquake data obtained from the BMKG website include coordinates, magnitudes, and earthquake depths recorded between 1 January 2008 and 28 February 2023. The free-air gravity anomaly data from the GGMplus website (https://ddfe.curtin.edu.au/models/GGMplus/) include longitude, latitude, and free-air anomaly values. Additionally, topographic data from the ERTM dataset, provided by Curtin University, complements the GGMplus data.

COMPLETE BOUGUER ANOMALY (CBA)

The data used in CBA processing are derived from free-air anomaly data obtained from the GGMplus.The CBA is obtained by applying Bouguer and terrain correction to the free-air anomaly data. The CBA is calculated using the formula provided in Equation (1):

$$CBA = FAC - BC + TC \quad (1)$$

where *CBA* is Complete Bouguer Anomaly (mGal); *FAC* is free-air anomaly (mGal); *BC* is Bouguer Correction (mGal); and *TC* is Terrain Correction (mGal) (Eleonora et al. 2023; Telford, Geldart & Sheriff 1990). *CBA* is a collection of regional anomaly responses and residuals. Upward Continuation is one method of separating regional and residual anomalies by removing local effects (Indriana, Nurwidyanto & Laode 2020). The upward equation is written in Equation (2):

$$U(x', y', z_0 - h) = \int_{-\infty}^{\infty}\int_{-\infty}^{\infty} \frac{h}{2\pi\{(x-x')^2 + (y-y')^2 + h^2\}^{\frac{3}{2}}} U(x, y, z_0)\,dx\,dy \quad (2)$$

with $x', y', z_0 - h$ are the total potential field at a point that is in the Upward Continuation plane with a height of *h* to the surface plane (measurement plane), where the field large is $U(x, y, z_0)$ which has been known. $U(x, y, z_0)$ is the complete Bouguer anomaly (Indriana, Nurwidyanto & Widada 2021). The residual gravity anomaly is simply the difference between the *CBA* and the regional field obtained by upward continuation:

$$Residual = U(x, y, z_0) - U(x', y', z_0 - h) \quad (3)$$

b-VALUE AND *a*-VALUE

The calculation of the *b*-value and *a*-value is performed by dividing the calculation area into regular grids. The size and number of grids are adjusted based on the area to be analyzed. The study area is divided into 16 grids, and the dimensions are 0.19° × 0.14°. The calculation of the *b*-value and *a*-value for each grid uses the equation relating magnitude to the logarithm of cumulative frequency, as shown in Equation (4):

$$Log\, N\,(M_C) = a - bM \quad (4)$$

where $N(M_C)$ is the number of earthquakes with magnitude $\geq M_C$; *a* represents the spatial characteristic parameter; *b* denotes the regional characteristic parameter, and M is the magnitude (Gutenberg & Richter 1944). The *a*-value indicates the seismic activity level of a region. The *a*-value indicates the total number of earthquakes occurring over a time and area. The *b*-value functions as a proxy for crustal stress conditions, with higher values generally reflecting a heterogeneous lithology, elevated thermal gradients, increased pore fluid pressures, or relatively low differential stress. Conversely, lower *b*-values are typically associated with more uniform, brittle rock compositions under high differential stress, conditions that have been linked to the increased likelihood of large-magnitude seismic events.

The linear relationship between magnitude and the frequency logarithm (Gutenberg-Richter theory) generally exhibits a consistent level of repeatability within a given earthquake region (Sochaimi 2008). The relationship between magnitude and the logarithm of cumulative frequency is solved using the least squares method, as expressed in Equation (5):

$$Y = a + bX \quad (5)$$

where *Y* is the response variable; *X* is the independent variable; and *a* and *b* are constants. The dependent variable (*Y*) corresponds to the logarithm of the cumulative number of earthquakes ($Log\, N\,(M_C)$), which represents the frequency of seismic events. The independent variable (*X*) is the earthquake magnitude (*M*), which serves as the predictor for changes in earthquake frequency across different magnitudes.

The values of *a* and *b* are determined using Equations (5) and (6) (Montgomery, Peck & Vining 2012):

$$b = \frac{n\sum(X_i \cdot Y_i) - (\sum(X_i) \cdot (\sum Y_i)}{n\sum X_i^2 - (\sum X_i)^2} \quad (6)$$

$$a = \frac{n\sum Y_i - b\sum X_i}{n} \quad (7)$$

The *a* -value, as derived from Equation (7), reflects the general seismicity level within a specific region or grid cell. The high *a* -values are indicative of regions experiencing a larger total number of seismic events across the full magnitude range, typically corresponding to areas with high tectonic activity. In contrast, lower *a*-values characterize

regions with fewer recorded earthquakes, often associated with tectonically stable or seismically quiet environments.

The *b*-value, determined through Equation (6), characterizes the proportional distribution between small and large earthquakes. Higher *b*-values (> 1) suggest a predominance of smaller magnitude events, frequently linked to reduced differential stress, elevated temperatures, or increased geological heterogeneity. Conversely, lower *b*-values (<1) imply a comparatively greater occurrence of larger magnitude earthquakes, generally associated with uniform, brittle rock formations subjected to high differential stress. Such low *b*-value regions have also been considered as potential indicators of areas susceptible to future large seismic events.

SEISMIC MOMENT

Seismic moment is the level of earthquake strength, based on changes in rock stress caused by fault movement. It is also used to describe the state of rock stress (Aki 1966; Kanamori & Brodsky 2004). The seismic moment equation is presented by Equation (8) as follows:

$$M_0 = \mu D\, c^a \tag{8}$$

where M_0 is the seismic moment (Nm); μ is rigidity (Pa); a is the area of the fault plane (m^2); and Dc is the average displacement of the fault plane (m). The seismic moment can also be calculated using the relationship between magnitude and seismic moment if the magnitude is known, as in the equation:

$$Log\, M_0 = 1{,}5M + 9{,}1 \tag{9}$$

with M is magnitude (SR) (Kanamori & Brodsky 2004).

The processing results are spatial variation maps of the *b*-value and *a*-value. The *b*-value indicates rock fragility, while the *a*-value represents spatial seismicity. The spatial variation maps of seismic moment, which defines the seismic moment reflect the level of stress in the rocks. The last is residual anomaly maps of gravity data, which illustrate variations in the density of subsurface rocks.

RESULTS AND DISCUSSION

The calculation of values *a* and *b* is based on 16 blocks. Figure 2(a) shows an example of the calculation results of *a* value and *b* value obtained from the graph. The result of seismic data processing is the *b*-value distribution map of the Cianjur area (Figure 2(b)), which maps *b*-value values from 0.25 to 1.00. The highest values, between 0.50 and 1.00, are observed in Cianjur Regency. Previous studies reported similar *b*-values ranging from 0.25 to 1.00 (Ernandi 2020; Nuannin, Kulhanek & Persson 2005). The southeast, southwest, and northwest areas have lower *b*-values, between 0.25 and 0.36. Other regions have intermediate values of 0.37 to 0.62. The *b*-value is used to determine the ratio between small earthquakes and large earthquakes. If $b > 1$, more small earthquakes occur than large earthquakes (low-stress zone). If $b < 1$, larger earthquakes occur (high-stress zone), and there is potential for large earthquakes (Allen 1986). This research area has a *b*-value >1, so small earthquakes have a lot of potential. Notably, high *b*-values are observed around Mt. Pangrango, Mt. Gede, and Mt. Salak, suggesting increased rock fragility in these areas. In contrast, regions with low *b*-values, including parts of Bogor Regency and the western Sukabumi Regency, are characterized by reduced rock fragility. According to the theory proposed by Gutenberg and Richter (1944), *b*-values are correlated with the structural characteristics of rock formations, making them valuable for understanding seismic activity in a region. The findings indicate that the Cianjur area and its surroundings are vulnerable to seismic activity.

a-value is used to determine how active a seismic zone is and helps in mapping the earthquake potential of an area. The *a*-value distribution map (Figure 2(b)) follows a similar spatial pattern to the *b*-value map, with values ranging from 1.1 to 3.7. The highest *a*-values, between 3.3 and 3.7, are located in Cianjur Regency, near Mt. Pangrango, and around Mt. Salak, indicating high seismic activity. Conversely, areas with lower *a*-values, ranging from 1.1 to 2.1, are found in the southeast, southwest, and northwest of the study area. Intermediate *a*-values, between 2.1 and 2.8, are distributed across other regions. *a*-value represents the level of seismic activity, which depends on the study area and observation period (Prananda, Zera & Sunarya 2022).

Regions with high *a*-values, such as the vicinity of Mt. Pangrango and Mt. Salak, experience frequent earthquakes. Meanwhile, regions with low *a*-values, such as Bogor City, Bogor Regency, and Sukabumi Regency, are characterized by lower seismic activity. The west of Mt. Pangrango-Gede and the east of Mount Salak have the highest *a*-value, so this area can have many earthquakes or become a high seismicity zone (Widiyantoro et al. 2020).

The seismic moment is a measure of the total energy released by an earthquake. Seismic moment measures the amount of earthquake energy more accurately than magnitude. Seismic moments are used in tectonic studies to understand fault mechanisms and the potential for large earthquakes. Seismic moment calculations are more stable than local magnitudes in determining the size of large earthquakes (Rohadi, Grandis & Ratag 2014).

The results of the seismic moment calculations show values ranging from 12.28 to 14.70, as shown in Figure 2(b). The lowest seismic moment values (12.28-12.74) are found in Cianjur Regency, particularly near Mt. Pangrango. The low seismic moment is in the west of Mt. Pangrango - Mt. Gede, which shows that the energy released is not large when an earthquake occurs, so the earthquake that might occur is small. This indicates low rock stress levels, leading to frequent small-magnitude earthquakes in this region. In contrast, the highest seismic moment values (13.70-14.70)

occur in the southeast, southwest, and northwest, indicating higher rock stress levels. Areas with medium seismic moment values (12.75-13.69) are distributed across the rest of the study area. Regions such as Bogor City, Bogor Regency, and Sukabumi exhibit high seismic moment values, highlighting areas of significant rock stress. These variations in value indicate the relationship between rock stress and seismic activity across the study area.

Figure 3 is a graph of the *a*-value, b-value, and seismic moment of 16 blocks. *a*-value and *b*-value have almost the same pattern. The seismic moment graph is opposite to the *a*-value and *b*-value graph. When the *a*-value and *b*-value are high, the seismic moment is low, and vice versa. Areas with more fragile rocks tend to have a high *a*-value, as there are more small earthquakes due to localized cracks and failures. The *b*-value indicates the ratio of large and small earthquakes. More fragile rocks usually have a higher *b*-value because small cracks occur more often before reaching a major failure. Stronger and more compact rocks have a lower *b*-value, which means more large earthquakes than small ones. The *b*-value is also affected by pressure and temperature. In the shallow crust, where rocks are more brittle, the *b*-value tends to be higher, whereas in the deep crust or upper mantle, where deformation is more plastic, the *b*-value is lower because more energy is released through fewer large earthquakes.

Areas with frequent small and fewer large earthquakes tend to have a steeper frequency-magnitude curve,

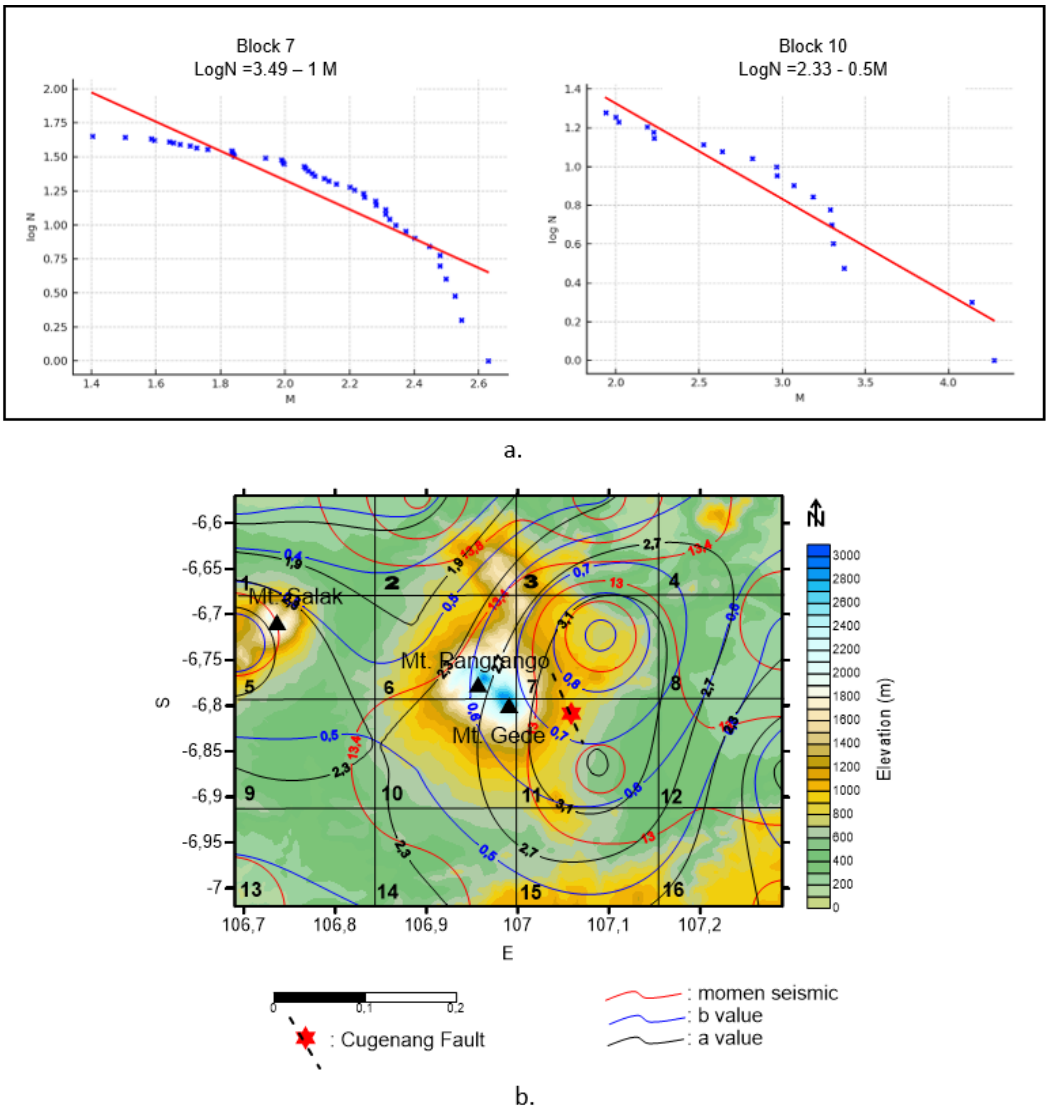

FIGURE 2. a) Linear equation for *a*-values and *b-values* derived from $LogN(M_c) = a - bM$,and b) Moment seismic, *a*-value, and *b*-value map of 16 blocks on topographic

resulting in higher *b*-values (Linda, Ihsan & Palloan 2019). Conversely, lower *b*-values are associated with high shear stress on rocks. The seismic moment describes the stress state of rocks and is directly proportional to earthquake magnitude, serving as a measure of earthquake strength (Aki 1966). Areas with a lower average earthquake magnitude will exhibit lower seismic moments, and vice versa. Regions with low seismic moments experience low levels of rock stress due to the limited displacement along fault planes and smaller fault plane areas (Kanamori & Brodsky 2004). A seismic moment is a level of the earthquake energy, released by rocks when they fail to resist stress. If a region has a low *b*-value, more energy is stored until released in a large earthquake, resulting in a high seismic moment. If the *b*-value is high, the energy is released in many small earthquakes, resulting in a more distributed total seismic moment. Brittle rocks are more prone to cracking and failure, resulting in small earthquakes (high *b*-value). Stronger, more ductile rocks tend to undergo longer elastic deformation before failing suddenly, resulting in more frequent large earthquakes (low *b*-value). Deeper tectonic zones often have ductile rock due to high stress, causing fewer large earthquakes than the more brittle shallow crust. So, brittle rocks tend to have higher *b*-values and more small earthquakes, while strong rocks tend to have lower *b*-values and more large earthquakes with high seismic moments.

Bouguer anomaly processing uses GGmPlus secondary data so that the corrections applied are Bouguer and terrain corrections. Processing was carried out using commonly used methods and gravity data processing and obtained Bouguer correction results of 7.49 mGal to 334.883 mGal and Terrain correction of 0.35 mGal - 52.39 mGal. Bouguer correction processing produces a simple Bouguer anomaly of -27.18 mGal - 139.54 mGal, while the complete Bouguer anomaly value obtained is 25 mGal to 145 mGal. The maximum *CBA* values are in the southwest, marked in red, while the minimum values are concentrated in the Mt. Gede – Pangrango area to the east of the study area, marked in purple (Figure 4). The *CBA* values decrease toward the north. Geologically, the northern part of Java Island was formed through volcanic activity resulting from plate subduction in the southern Java region. The southern part of West Java is hypothesized to have a rock composition with higher density than that of the northern part. The *CBA* values obtained reflect a combination of regional and local responses. Understanding the local response is essential for identifying density variations in shallow zones (Telford, Geldart & Sheriff 1990).

The separation process of the local anomalies from the regional response used the Upward Continuation method. The results of this separation provide a local anomaly map, which is presented in Figure 5. Low residual anomaly -16 mGal - 1 mGal, trending east-west across the Mt. Gede-Pangrango and Mt. Salak areas. Residual anomalies are moderate to high, 2 mGal - 26 mGal trending southeast to west and south.

This map is used to identify density variations in the shallow subsurface, offering insights into the geological structure of the study area. Areas with negative gravity anomalies tend to have a more heterogeneous density due to variations in rock composition, such as differences between the upper and lower crust or fault zones that have experienced intensive fracturing. In contrast, areas with positive gravity anomalies show more dense and homogeneous rocks, such as compact igneous or metamorphic rocks (Blakely 1996). Figure 5 shows a clear correlation between residual gravity anomalies, seismic

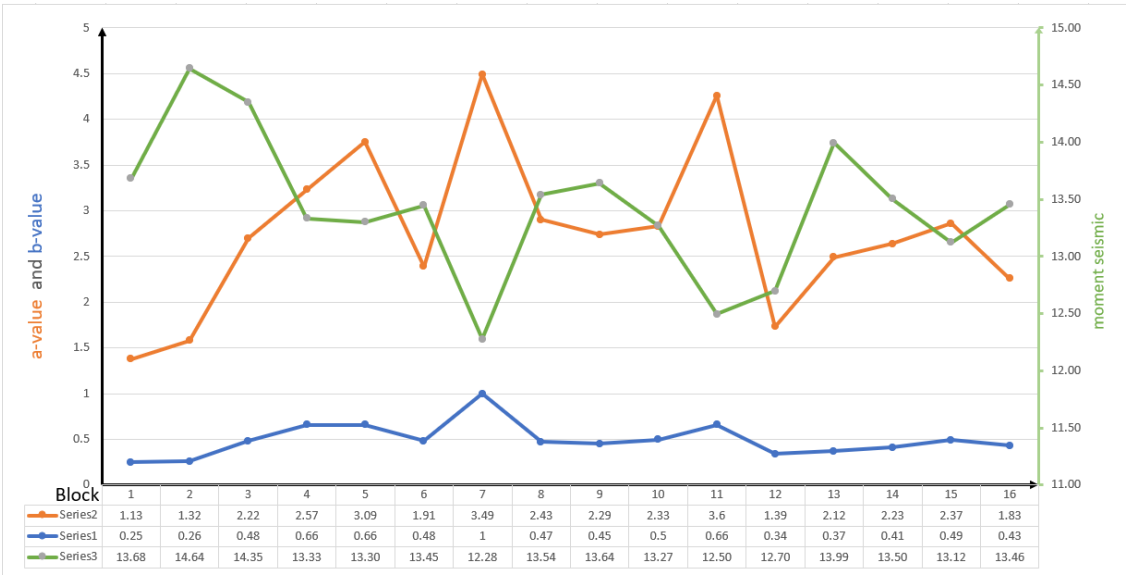

Block	1	2	3	4	5	6	7	8	9	10	11	12	13	14	15	16
Series2	1.13	1.32	2.22	2.57	3.09	1.91	3.49	2.43	2.29	2.33	3.6	1.39	2.12	2.23	2.37	1.83
Series1	0.25	0.26	0.48	0.66	0.66	0.48	1	0.47	0.45	0.5	0.66	0.34	0.37	0.41	0.49	0.43
Series3	13.68	14.64	14.35	13.33	13.30	13.45	12.28	13.54	13.64	13.27	12.50	12.70	13.99	13.50	13.12	13.46

FIGURE 3. Graphical *a*-value, *b*-value, and moment seismic on 16 blocks of data

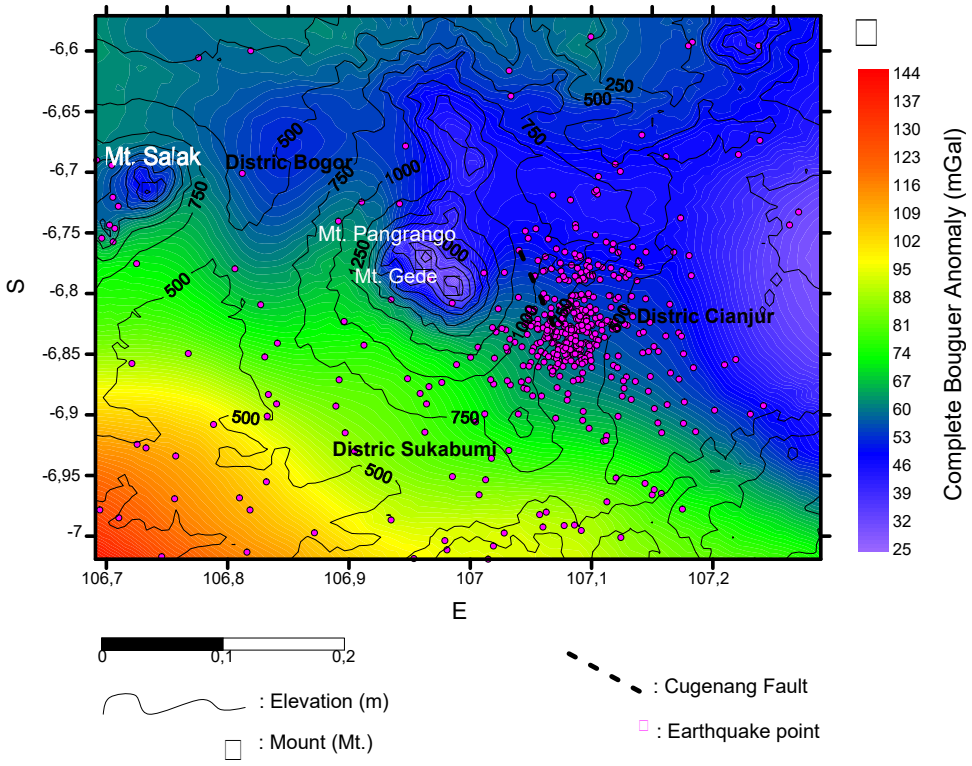

FIGURE 4. Complete Bouguer Anomaly on topography with earthquake point

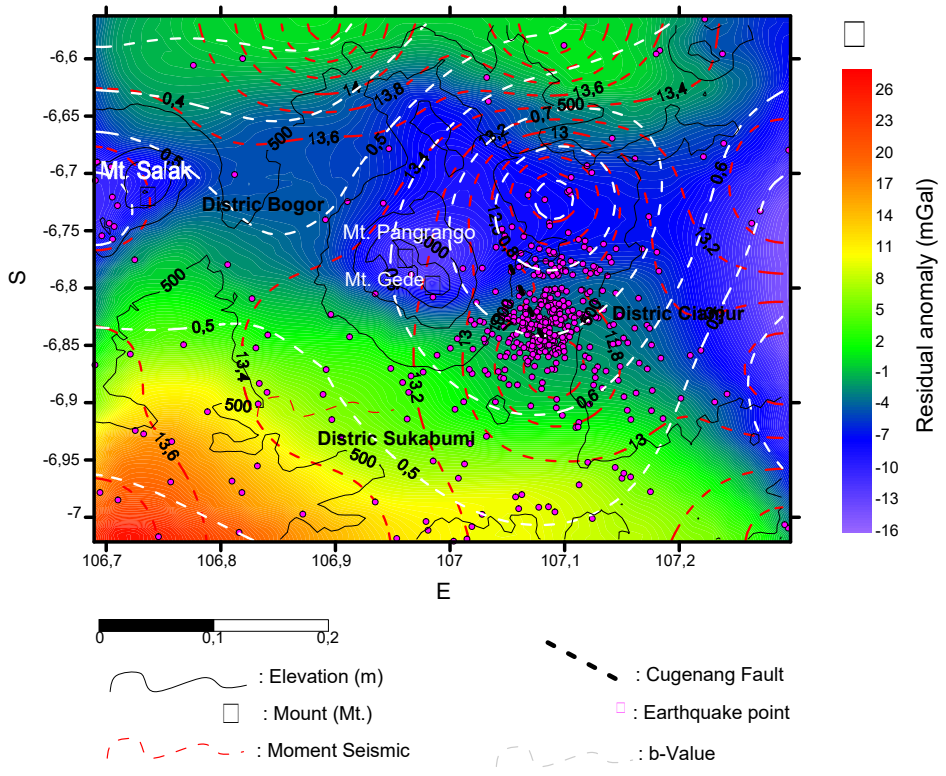

FIGURE 5. Residual Bouguer Anomaly mapped on topography with earthquake point, *b*-value contour, and moment seismic contour

moment, and *b*-values. Low residual gravity anomalies correspond to low seismic moments and high *b*-values, while high residual gravity anomalies correlate with high seismic moments and low *b*-values.

Residual gravity anomalies, *b*-values, and seismic moments are interrelated. Low residual gravity anomalies suggest rocks with low density. The analysis of residual Bouguer gravity anomalies in the Cianjur region resulted in anomaly variations of -10 to 28 mGal. The variations indicate short-wavelength density heterogeneity in shallow layers. The interpretation of residual anomalies was based on the lithology identified in the geological map of West Java. Lower residual gravity anomalies are concentrated in the upland zones of Mt. Gede, Pangrango, and Salak, coinciding with Quaternary volcanic rocks (Qv) and unconsolidated alluvial deposits. These lithologies are characterised by low bulk density (approximately 2.1-2.4 g/cm^3) due to their high porosity, weak compaction, and fragmental composition. In contrast, high residual gravity anomalies are found in the south-western part of the area, aligned with denser and more consolidated Miocene marine sedimentary rocks (Tms, Tom) and intrusive bodies (Ttv) (estimated at 2.6-2.9 g/cm^3). Qualitatively, the residual gravity anomalies may reflect variations in near-surface rock density.

Low residual gravity anomalies suggest rocks with low density in the survey area, which are brittle and sensitive to vibrations and stress. Brittle rocks, having low-stress levels, tend to release energy more easily, leading to frequent small-magnitude earthquakes. These conditions correspond to low seismic moments, high *b*-values, and high *a*-values. Conversely, areas with high residual gravity anomalies have denser rocks that are less brittle. Such rocks accumulate stress rather than releasing it frequently, resulting in infrequent but high-magnitude earthquakes. These characteristics are associated with high seismic moments, low *b*-values, and low *a*-values. Density variations have a significant influence on earthquake activity. High Bouguer gravity anomalies are associated with areas of low *b*-values and vice versa. High *b*-values correlate with frequent, small-magnitude earthquakes, whereas low *b*-values are linked to infrequent but large-magnitude earthquakes (Sarkarinejad, Zadeh & Webster 2013; Zamani & Hashemi 2000). This relationship aligns with findings by Khan and Chakraborty (2007) in the Shillong Plateau, where seismic moment and Bouguer gravity anomaly inversely relate to *b*-values. Similarly, research in the Indo-Burma region (northeast India) by Bora (2018) reported that high *b*-values are associated with negative gravity anomalies and low seismic moments. High *b*-values generally indicate relatively low-stress concentrations in the rocks (Bora 2018). The relationship between gravity anomaly, *a*-value, *b*-value, seismic moment, and the level of rock homogeneity is related to the physical and mechanical characteristics of the earth's crust around the New Cugenang Fault, which are a negative residual gravity anomaly, high *b*-value, high *a*-value, and low seismic moment. The Cugenang fault area is a wide fracture zone, a heterogeneous rock, which has low-stress/brittle characteristics, therefore, it cannot hold energy (Ahumada et al. 2022).

The areas with low residual anomalies, which are underlain by brittle and low-density rocks, show high *b*-values and high *a*-values. This indicates the dominance of small-magnitude and frequent seismic events. Brittle rocks release energy through micro-fractures, generating low seismic moments. In contrast, areas with high residual anomalies and denser lithologies show lower *b*-values and higher seismic moments. This requires greater energy accumulation, resulting in the potential for seismic events to occur with greater magnitude. Earthquake hypocentral depths are generally 0 to 30 km, while residual gravity anomalies are most sensitive to density variations at depths of 5-10 km. The residual anomaly, *b*-value, and seismic moment are not located at the same depth, but they provide complementary insights. Gravity anomalies provide information on shallow compositional variations, while *b*-values and seismic moments inform on deeper crustal stresses. The combined analysis of these geophysical indicators provides a coherent understanding of crustal structure and seismotectonic behaviour in the Cianjur region.

The earthquake distribution by magnitude is illustrated in Figure 6. The earthquake hypocentres in the study area are relatively shallow. The Cugenang Fault, identified by BMKG with a strike of N347° E, a steep dip of 82.8°, and a dextral strike-slip mechanism, lies at a depth of 10–11 km within the brittle upper crust. Its orientation reflects crustal adjustment to the oblique convergence between the Indo-Australian and Eurasian plates, which induces both compressional and strike-slip deformation across West Java's complex tectonic setting. This oblique stress is accommodated by active faults such as the Cimandiri and Cugenang Faults, trending NW–SE. The Cugenang Fault aligns with clusters of shallow earthquake epicenters (mostly <10 km), and its surface trace corresponds to zones of low residual Bouguer gravity anomalies, indicating low-density, fractured volcanic rocks typical of fault zones. High *a*-values and *b*-values (>1) in the region suggest frequent, low-magnitude seismicity in a heterogeneous, low-stress crust. Variations in seismic moment point to asperities capable of larger ruptures. Recent seismicity, concentrated north of the Rajamandala segment of the Cimandiri Fault, coincides with the Cugenang Fault, reinforcing its role as an active, previously unmapped structure. Although the region is dominated by Quaternary volcanic breccia, lava, lapilli, and tuff from Mt. Gede and Mt. Pangrango, PVMBG confirms that earthquakes here are tectonic, not volcanic. These weathered, fragile volcanic rocks contribute to the region's susceptibility to seismic failure. Thus, the combined gravity, geological, and seismic data confirm that the Cugenang Fault plays a significant role in accommodating oblique tectonic deformation in southern Java (Daryono 2022; Pepen et al. 2023; Prezzi et al. 2017).

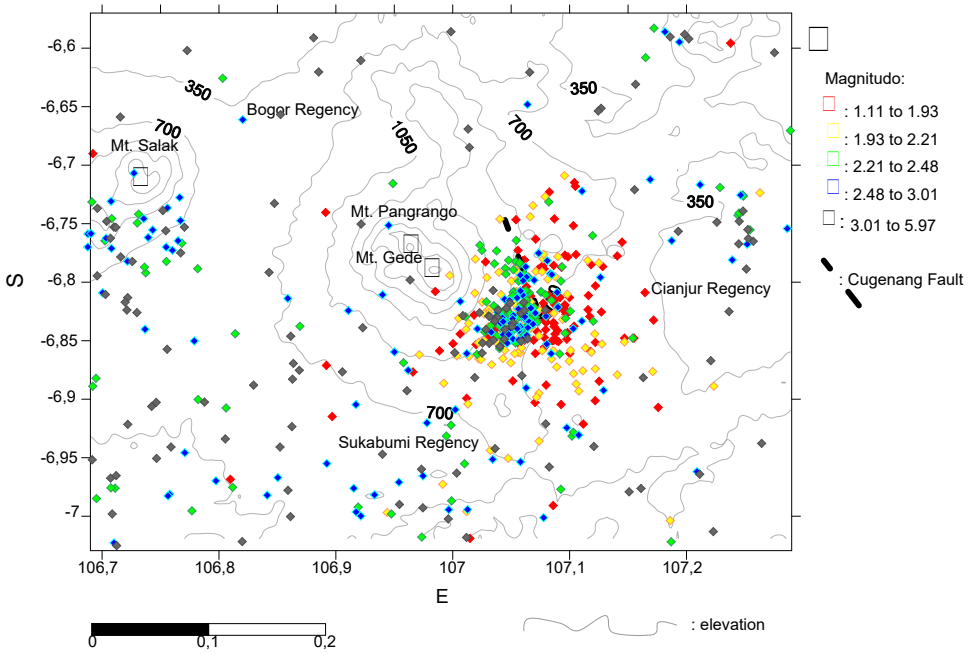

FIGURE 6. The earthquake magnitude map

CONCLUSIONS

The research findings indicate that the Cugenang-Cianjur earthquake is primarily tectonic, as suggested by the *b*-values (0.25-1.00), *a*-values (1.1-3.7), and seismic moment values (12.28-14.64). High *b*-values and *a*-values in the Cianjur region signify a high degree of rock fragility and seismicity. Conversely, low seismic moment values and residual gravity anomalies around Cianjur correlate with increased rock fragility in areas with homogeneous rock types. The relationship between gravity anomaly, *a*-value, *b*-value, seismic moment, and the level of rock homogeneity is related to the physical and mechanical characteristics of the earth's crust around the Ciguneng Fault, which are a negative residual gravity anomaly, high *b*-value, high *a*--value, and low seismic moment. The Cugenang fault area is a wide fracture zone, a heterogeneous rock, that has low-stress/brittle characteristics, so it cannot hold energy. The orientation of the Cugenang fault is N 347° E / 82.8°, depth 10 - 11 km, and a dextral strike-slip mechanism. Tectonic analysis reveals that the majority of earthquake epicenters are situated northern of the Cimandiri fault (Rajamandala segment) and directly at the Cugenang fault's location. Geologically, these areas are composed of young volcanic deposits, including volcanic breccia, lava, and tuff, which are fragile and not compact. The combination of active fault systems and brittle volcanic rocks makes the Cianjur region highly susceptible to seismic events. This vulnerability may lead to the development of new faults, further increasing the region's seismic risk.

ACKNOWLEDGMENTS

The authors would like to express sincere gratitude to the Meteorology, Climatology, and Geophysics Agency (BMKG) for their support and for providing the data of this research.

REFERENCES

Ahumada, M.F., Sanchez, M.A., Vargas, L., Filipovich, R., Martínez, P. & Viramonte, J.G. 2023. Joint interpretation of gravity and airborne magnetic data along the Calama-Olacapato-Toro fault system (Central Puna, NW Argentina): Structural and geothermal significance. *Geothermics* 107: 102597.

Aki, K. 1966. Earthquakes generating stress in Japan for the years 1961 to 1963 obtained by smoothing the first motion radiation patterns. *Bull. Earthq. Res. Inst.* 44: 447-471.

Allen, J.R.L. 1986. Earthquake magnitude-frequency, epicentral distance, and soft-sediment deformation in sedimentary basins. *Sedimentary Geology* 46(1-2): 67-75.

Blakely, R.J. 1996. *Potential Theory in Gravity and Magnetic Applications*. Cambridge: Cambridge University Press.

Bora, D.K., Borah, K., Mahanta, R. & Borgohain, J.M. 2018. Seismic b-values and its correlation with seismic moment and Bouguer gravity anomaly over Indo-Burma ranges of northeast India: Tectonic implications. *Tectonophysics* 728: 130-141.

Daryono. 2022. BMKG Report on the Cianjur Earthquake (M5.6, 21 November 2022).

Eleonora, A., Krishna, A.P., Muhammad, A.B., Mariyanto, Mimin, I., Cahyo A.H. & Rina, D.I. 2023. Identification of mud volcano's structure using gravity satellite and fault fracture density analysis: Case study Ciuyah Mud Volcano, Kuningan, West Java. *Sains Malaysiana* 52(11): 3013-3026.

Ernandi, F.N. 2020. Analisis variasi a-value dan b-value dengan menggunakan software zmap v. 6 sebagai indikator potensi gempa bumi di wilayah Nusa Tenggara Barat. *Inovasi Fisika Indonesia* 9(3): 24-30.

Gutenberg, B. & Richter, C.F. 1944. Frequency of earthquakes in California. *Bulletin of the Seismological Society of America* 34(4): 185-188.

Hilmi, I.L. 2019. Analisis seismisitas berdasarkan data gempa bumi periode 1958-2018 menggunakan b-value pada Daerah Selatan Jawa Barat dan Banten. Bachelor's Thesis, Fakultas Sains dan Teknologi UIN Syarif Hidayatullah Jakarta (Unpublished).

Hirt, C., Kuhn, M., Claessens, S., Pail, R., Seitz, K. & Gruber, T. 2014. Study of the Earth′ s short-scale gravity field using the ERTM2160 gravity model. *Computers & Geosciences* 73: 71-80.

Holtkamp, S. & Brudzinski, M.R. 2014. Megathrust earthquake swarms indicate frictional changes which delimit large earthquake ruptures. *Earth and Planetary Science Letters* 390: 234-243.

Indriana, R.D., Mariyanto, M., Agustin, E., Iryanti, M., Hapsoro, C.A., Koesuma, S. & Ashadi, A.L. 2024. Gravity interpretation of mud volcano based on satellite data (study case Kuwu and Cangkring mud volcano). *Indonesian Journal of Applied Physics* 14(1): 165-175.

Indriana, R.D., Nurwidyanto, M.I. & Widada, S. 2021. Remodeling Kaligarang fault based on satellite gravity data. *Journal of Physics: Conference Series* 1943(1): 012004.

Indriana, R.D., Nurwidyanto, M.I. & Laode, M.S. 2020. Data validation of gravity field and satellite data using correlation and coherence method. *Journal of Physics and Its Applications* 3(1): 113-119.

Kanamori, H. & Brodsky, E.E. 2004. The physics of earthquakes. *Reports on Progress in Physics* 67(8): 1429.

Khan, P.K. & Chakraborty, P.P. 2007. The seismic b-value and its correlation with Bouguer gravity anomaly over the Shillong Plateau area: Tectonic implications. *Journal of Asian Earth Sciences* 29(1): 136-147.

Linda, L., Ihsan, N. & Palloan, P. 2019. Analisis distribusi spasial dan temporal seismotektonik berdasarkan nilai b-value dengan menggunakan metode likelihood di Pulau Jawa. *Jurnal Sains dan Pendidikan Fisika* 8(3): 269-278.

Mogi, K. 1963. Some discussions on aftershocks, foreshocks and earthquake swarms-the fracture of a semi finite body caused by an inner stress origin and its relation to the earthquake phenomena. *Bull. Earthq. Res. Inst.* 41: 615-658.

Montgomery, D.C., Peck, E.A. & Vining, G.G. 2021. *Introduction to Linear Regression Analysis*. New Jersey: John Wiley & Sons.

Murjaya, J. 2021. Tatanan tektonik dan implikasi kegempaan di Pulau Jawa Bagian Barat dan sekitarnya. *Pusat Penelitian dan Pengembangan BMKG*.

Nuannin, P., Kulhanek, O. & Persson, L. 2005. Spatial and temporal b value anomalies preceding the devastating off coast of NW Sumatra earthquake of December 26, 2004. *Geophysical Research Letters* 32: L11307.

Pepen, S., Tom, W., Nicholas, R., Conor, A.B., Kadek, H.P., Andrean, S., Andri, K., Sri, W., Andri, D.N., Hasbi, A.S., Ardiantoe, Daryono, Suko, P.A., Dwikorita, K., Priyobudi, Gayatri, I.M., Iswandi, I. & Jajat, J. 2023. Fault zone structure and damage related to the 2022 Cianjur Earthquake inferred from aftershock distribution. *Earth, Planets and Space* 75: 64.

Prananda, Y., Zera, T. & Sunarya, D. 2022. Analisis distribusi spasial dan temporal parameter seismotektonik wilayah Jawa Barat dan Banten berdasarkan a-value dan b-value periode 1971-2021. *Buletin Meteorologi, Klimatologi dan Geofisika* 2(3): 24-34.

Prezzi, C., Risso, C., Orgeira, M.J., Nullo, F., Sigismondi, M.E. & Margonari, L. 2017. Subsurface architecture of Las Bombas volcano circular structure (Southern Mendoza, Argentina) from geophysical studies. *Journal of South American Earth Sciences* 77: 247-260.

Ratman, N. & Gafoer, S. 1998. *Peta Geologi Lembar Jawa Bagian Barat Edisi Kedua Skala 1:500.000*. Bandung: Pusat Peneltian dan Pengembangan Geologi.

Rohadi, S., Grandis, H. & Ratag, M.A. 2017. Studi variasi spatial seismisitas zona subduksi Jawa. *Jurnal Meteorologi dan Geofisika* 8(1): 42-47.

Sarkarinejad, K., Zadeh, R.M. & Webster, R. 2013. Two-dimensional spatial analysis of the seismic b-value and the Bouguer gravity anomaly in the southeastern part of the Zagros Fold-and-Thrust Belt, Iran: Tectonic implications. *Journal of Asian Earth Sciences* 62: 308-316.

Scholz, C.H. 1968. The frequency-magnitude relation of microfracturing in rock and its relation to earthquakes. *Bulletin of the Seismological Society of America* 58(1): 399-415.

Shohaya, J.N., Chasanah, U., Mutiarani, A., Wahyuni, L. & Madlazim, M. 2013. Survey dan analisis seismisitas Wilayah Jawa Timur berdasarkan data gempa bumi periode 1999-2013 sebagai upaya mitigasi bencana gempa bumi. *Jurnal Penelitian Fisika dan Aplikasinya (JPFA)* 3(2): 18-27.

Soehaimi, A. 2008. Seismotektonik dan potensi kegempaan wilayah Jawa. *Indonesian Journal on Geoscience* 3(4): 227-240.

Telford, W.M., Geldart, L.P. & Sheriff, R.E. 1990. *Applied Geophysics*. Cambridge: Cambridge University Press.

Visser, S.W. 1922. *Inland and Submarine Epicentra of Sumatra and Java Earthquakes*. Batavia: Javasche Boekhandel en Drukkerij.

Widiyantoro, S., Gunawan, E., Muhari, A., Rawlinson, N., Mori, J., Hanifa, N.R., Susilo, S., Supendi, P., Shiddiqi, H.A., Nugraha, A.D. & Putra, H.E. 2020. Implications for megathrust earthquakes and tsunamis from seismic gaps south of Java Indonesia. *Scientific Reports* 10: 15274.

Wiemer, S., McNutt, S.R. & Wyss, M. 1998. Temporal and three-dimensional spatial analyses of the frequency–magnitude distribution near Long Valley Caldera, California. *Geophysical Journal International* 134(2): 409-421.

Zamani, A. & Hashemi, N. 2000. A comparison between seismicity, topographic relief, and gravity anomalies of the Iranian Plateau. *Tectonophysics* 327(1-2): 25-36.

*Corresponding author; email: rinadwiindriana@lecturer.undip.ac.id